Molecular Cell, Vol. 2, 247–251, August, 1998, Copyright ©1998 by Cell Press

Somatic Mutation in Individual Liver Cysts Supports a Two-Hit Model of Cystogenesis in Autosomal Dominant Polycystic Kidney Disease

Terry J. Watnick,* Vicente E. Torres,† Michael A. Gandolph,* Feng Qian,* Luiz F. Onuchic,* Katherine W. Klinger,‡ Gregory Landes,‡ and Gregory G. Germino*§

*Division of Nephrology
The Johns Hopkins University School of Medicine
Baltimore, Maryland 21205
†Division of Nephrology
Mayo Clinic
Rochester, Minnesota 55905
‡Genzyme Corporation
Framingham, Massachusetts 01701

Summary

Autosomal dominant polycystic kidney disease (ADPKD), Type I is a common genetic disorder and an important cause of renal failure. The disease is characterized by progressive cyst formation in a variety of organs including the kidney, liver and pancreas. We have previously shown that in the case of *PKD1*, renal cyst development is likely to require somatic inactivation of the normal allele coupled to a germline *PKD1* mutation. In this report, we have used unique reagents to show that intragenic, somatic mutations are common in hepatic cysts. All pathogenic mutations were shown to have altered the previously normal copy of the gene. These data extend the "two-hit" model of cystogenesis to include a second focal manifestation of the disease.

Introduction

Autosomal dominant polycystic kidney disease (ADPKD) is a common genetic disorder with a prevalence at birth estimated to be 1:400–1:1000 (Iglesias et al., 1983; Gabow, 1993). Mutations in the *PKD1* gene on chromosome 16 account for ~85%–95% of clinically recognized cases, while the remainder are largely caused by mutations in *PKD2* on chromosome 4 (Peters and Sandkuijl, 1992; The European Polycystic Kidney Disease Consortium, 1994; The American PKD1 Consortium, 1995; Mochizuki et al., 1996). Renal cyst formation is a universal feature and leads to renal failure in approximately 50% of disease gene carriers. In addition, affected individuals may exhibit a variable combination of extrarenal manifestations including hepatic and pancreatic cysts, cerebral aneurysms, and cardiac valvular abnormalities (Iglesias et al., 1983; Kaehny and Everson, 1991; Everson, 1993; Gabow, 1993). A common feature of each of these findings is that they result from a focal process involving only a subset of cells in each of the target organs. This observation suggests that a second, possibly rate-limiting, step might be required for the pathogenic changes to occur in each tissue.

Recent studies by our group and others have provided one possible explanation for the focal nature of renal cyst formation (Qian et al., 1996; Brasier and Henske, 1997). We observed loss of heterozygosity (LOH) for 16p13.3 markers in epithelial cells lining individual renal cysts. In all cases where it could be determined, it was the normal haplotype that was lost. These data suggested that renal cyst development was likely to require somatic inactivation of the normal allele coupled to a germline *PKD1* mutation. This conclusion has been challenged by some investigators, however, because of the relatively low rate of detection of LOH (~20% of cysts) (Ong and Harris, 1997). It has been argued that the phenomenon might be a consequence of epithelial cell proliferation rather than an important step in cyst pathogenesis. Moreover, it has been noted that somatic deletions that cause LOH are likely to result in loss of the neighboring *TSC2* gene. Since germline mutations of *TSC2* have also been associated with renal cystic disease (Brook-Carter et al., 1994), it was suggested that somatic involvement of *TSC2* might be critical in the process of cystogenesis (Ong and Harris, 1997).

In the current report, we have examined the genetic basis of hepatic cyst formation in ADPKD. We have used novel methods to identify somatic mutations involving the normal *PKD1* allele in the epithelial cells lining individual hepatic cysts. As predicted, the mutations were discovered within the portion of the gene that is duplicated and thus inaccessible for analysis using conventional approaches. These data suggest that the two-hit model appears to hold true for a second focal manifestation of human ADPKD, and support our original hypothesis that ADPKD is likely to be recessive on a molecular level.

Results and Discussion

To examine the genetic basis of liver cyst formation, DNA was isolated from the liver cysts of two donors, JHU415 (12 cysts) and JHU452 (9 cysts). Techniques designed to maintain cyst wall integrity and to minimize contamination from surrounding cells were employed (Qian et al., 1996). The donors were then screened for the presence of polymorphisms at two well-characterized intragenic loci, *KG8* and *EJ1*, that could be used to test the cysts for loss of heterozygosity (LOH) (Figure 1) (Snarey et al., 1994; Qian et al., 1996). The first donor, JHU415, was informative only at *EJ1* while JHU452 was uninformative for both markers (data not shown).

Heteroduplex analysis of *EJ1* for liver cysts from JHU415 is shown in Figure 2A and demonstrates LOH for this marker in cysts (C) 8 and 12. Mixing studies using defined cloned alleles (A1–A3) suggested that both cysts with LOH lacked the A1 allele and that the remaining allele was neither A2 nor A3 (Figure 2B). This was confirmed by determining the sequence of cloned *EJ1* alleles from the blood sample of JHU415. As predicted, in addition to A1, JHU415 was found to contain a C-to-G transversion in exon 45 (cDNA base pair 12589, GenBank accession number L33243) that creates a premature stop codon and a new *Mae*I site. This germline

§To whom correspondence should be addressed (e-mail: ggermino@welchlink.welch.jhu.edu).

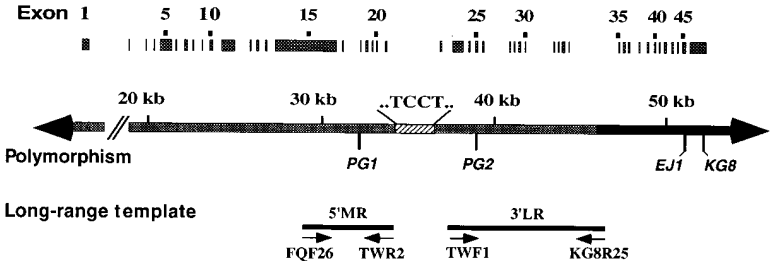

Figure 1. Genomic Structure of the *PKD1* Gene

The *PKD1* gene contains 46 exons and is bisected by a polypyrimidine tract of ~2.5 kb (hatched box). The replicated portion of the gene begins in exon 1 and ends in intron 34 (stippled bar). The locations of polymorphisms used for LOH studies and haplotype analysis are indicated. The positions of *PKD1*-specific, long-range PCR products, 3′LR (~10 kb) and 5′MR (~3 kb), are shown along with the primers used for amplification.

mutation, which was also present in an affected sibling (data not shown), is predicted to result in a truncated protein lacking the intracytoplasmic coiled-coil portion of the *PKD1* gene. This domain is functionally important because it is thought to mediate binding to the *PKD2* gene product (Qian et al., 1997; Tsiokas et al., 1997).

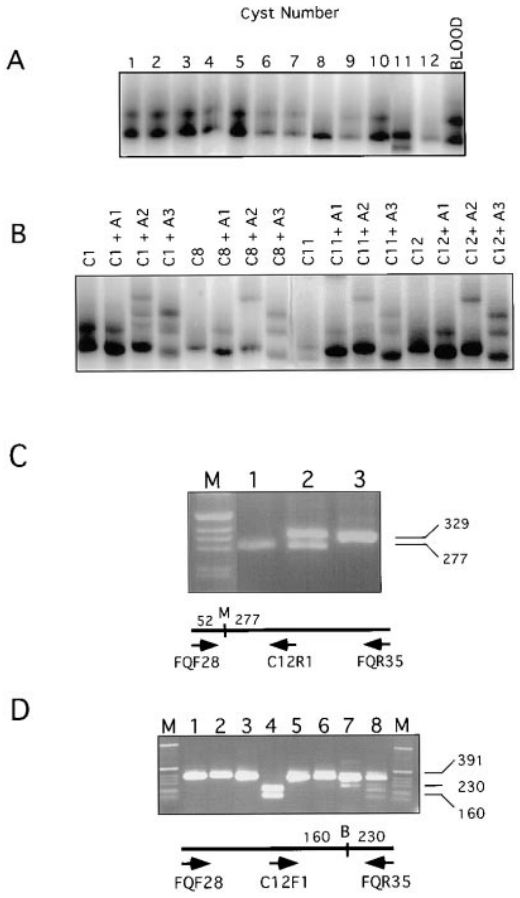

Figure 2. Loss of Heterozygosity (LOH) for *EJ1* in Cysts from Liver Donor JHU415

(A) *EJ1* was amplified from the blood of JHU415 as well as DNA isolated from 12 liver cysts and subjected to heteroduplex analysis. The majority of cysts (C) have the same pattern as the blood. C8 and C12, however, demonstrate LOH since heteroduplex formation is no longer seen. C11 shows a novel heteroduplex pattern.

(B) Mixing studies were performed to determine which *EJ1* allele remained in cysts with either LOH (C8, C12) or a novel heteroduplex pattern (C11). A cyst sample, C1, with a pattern representative of blood was included as a control. Unlabeled *EJ1* alleles A1, A2, and A3 were mixed separately with radiolabeled *EJ1* that was amplified from each cyst. The mix was analyzed for heteroduplex formation. The addition of A1 to the control cyst did not alter the preexisting heteroduplex pattern, while it restored the control pattern in C8 and C12. Addition of A2 and A3 to each cyst produced novel heteroduplex patterns. C11 exhibited mixing patterns similar to those of C8 and C12 but there were also new bands at the top of the gel that are not shown.

(C) A fragment of *EJ1* (FQF28-C12R1) was amplified from the blood of JHU415 and C12 and digested with MaeI. Both uncut (normal) and cut (mutant) products are present in the blood of JHU415 (lane 2), while only the cut product (mutant) remains in C12 (lane 1). A similar result was obtained for C8 (data not shown). Lane 3 shows the undigested product from blood. A restriction map, along with the relative position of primers used for amplification, is shown. The 52 bp fragment is not shown.

(D) A fragment of *EJ1* (C12F1-FQR35) was amplified from a clone containing the normal allele (lanes 1 and 2), a clone containing the 2 bp insertion (lanes 3 and 4), the blood of JHU415 (lanes 5 and 6), and C11 (lanes 7 and 8). Undigested products (lanes 1, 3, 5, and 7) and products digested with BstUI (lanes 2, 4, 6, and 8) are analyzed on a Nusieve gel. A *Bst*UI restriction map is shown along with the approximate position of the primers used to amplify the subfragment of *EJ1*. (M) represents the marker lane.

Once the germline mutation was identified, it was possible to confirm by restriction digest that this was the only allele remaining in both cysts with LOH (Figure 2C).

Interestingly, one additional cyst (Figure 2A, C11) from liver donor JHU415 demonstrated an unusual *EJ1* heteroduplex pattern. We cloned *EJ1* from this cyst and two distinct classes of clones were identified by sequencing. One group had the germline stop codon (N = 5), while the other contained a 2 bp (base pair) (GC) insertion (Table 1) that is predicted to result in a truncated protein after the addition of 12 novel amino acids (N = 5). The insertion creates a new *Bst*UI site that is present in the cyst sample but not in the donor's blood DNA (Figure 2D). Taken together, these data indicate that C11 has acquired a unique somatic mutation on the normal haplotype.

Since the second donor, JHU452, was uninformative for both *KG8* and *EJ1*, we decided to screen this individual for additional intragenic polymorphic markers that could be used to test for LOH. We chose to focus on the 5′ region of the gene since we had small quantities of cyst DNA and previous mutation studies suggested that this area is likely to harbor most of the sequence variation (Peral et al., 1996). Until recently, analysis of this portion of *PKD1* was virtually impossible since ~70% of the gene, from exon 1 to exon 34 (Figure 1),

Table 1. Somatic Mutations of PKD1 in Cystic Livers

Liver	Cyst#	Mutation	Location	Restriction Site Created	Predicted Effect
JHU415	8	LOH	Not defined	—	Loss of normal allele
	11	12,762insGC	Exon 46	*Bst*UI	Frameshift
	12	LOH	Not defined	—	Loss of normal allele
JHU452	2	C9111G	Exon 24	*Hinf*I	S2967X
	4	41,955del20	Exon 30/Intron 30	—	Consensus splice site disrupted
	6	T8769C	Exon 23	*Sfa*NI	F2853S
	8	G7778T	Exon 19	*Mae*I	E2523X
	9	8944del16	Exon 23	—	Frameshift

is present in multiple highly homologous copies on chromosome 16 (Germino et al., 1992; The European Polycystic Kidney Disease Consortium, 1994). We have developed a novel strategy for mutation analysis in the duplicated region of *PKD1* that allows us to circumvent the difficulties posed by the homologous loci (Watnick et al., 1997). Our method uses gene-specific primers located in two areas of *PKD1* to amplify large segments of the gene that can be used for mutation studies. We were able to use two of these *PKD1*-specific templates (3′LR and 5′MR, Figure 1) amplified from the blood DNA of JHU452 to screen exons 16–34 (excluding exon 22) via heteroduplex analysis. Two sequence variants were identified in the germline of JHU452. The first, *PG1*, is a silent T-to-C transition (T7376C) in exon 17 that is found in ~25% of normal samples (data not shown). The second variant (*PG2*) is located in exon 25 and is predicted to lead to a nonconservative amino acid change, substituting glutamine for arginine (A9258G, Q3016R). This latter change was not found in a screen of 100 normal chromosomes (data not shown). Pedigree analysis indicates that both *PG1* and *PG2*, which can be assayed by restriction digest, segregate with the disease phenotype in the family of JHU452 (Figure 3).

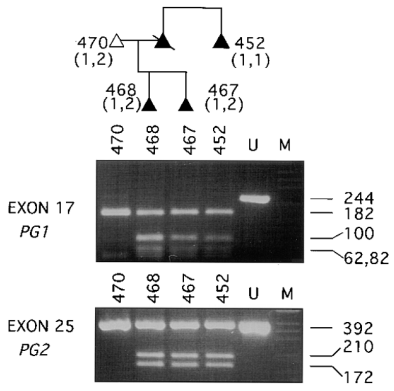

Figure 3. Exon 17 and Exon 25 Polymorphisms (*PG1* and *PG2*, Respectively) Segregate with ADPKD in the Family of JHU452

Exons 17 and 25 were amplified from the diluted 5′MR or 3′LR, respectively, of each family member and subjected to restriction digest with MvaI (exon 17) or MspI (exon 25). MvaI digest of exon 17 creates two new fragments of 100 and 82 bp in each affected family member. MspI digest cleaves the PCR product once, creating fragments of 210 and 172 bp in affected family members. All family members, regardless of sex, are represented by triangles. Closed triangles represent affected individuals. The numbers in brackets are the *KG8* alleles. (U) represents the uncut PCR product.

Although none of the 9 cysts demonstrated LOH for either of these intragenic markers, mutation analysis using 3′LR and 5′MR amplified from cyst DNA revealed unique heteroduplex patterns in five cysts. Each variant was sequenced and the results are summarized in Table 1. Two cysts contained intragenic deletions, one in exon 23 and the other in exon 30. The deletion in exon 30 was predicted to disrupt a consensus splice donor site (Figure 4). In addition, three cysts were found to have single base pair changes. Two of these were predicted to result in nonsense mutations in exons 19 and 24. The third was a nonconservative amino acid change in exon 23. In each case, the "mutation" was shown to be absent from the germline of JHU452 (*PKD1* and homologs), indicating that these changes were independent somatic events (data not shown).

The informative polymorphisms in exons 17 (*PG1*) and 25 (*PG2*) were then used to establish the haplotype for each pathogenic sequence variant (deletions and stop codons) using a variety of techniques. For the C8 stop codon in exon 19, a fragment linking exon 17 to 19 was amplified and cloned from an appropriately diluted long-range template. Nine clones were analyzed for the presence of *PG1* and the exon 19 stop codon. Clones contained either the stop codon or *PG1* but not both. The remaining cysts were analyzed using primers that could distinguish between mutant and normal alleles. PCR products were amplified directly from cyst DNA using an allele-specific primer in combination with an exon 25 primer and then tested for the absence or presence of *PG2* by MspI digestion. Characterization of the exon 30 deletion is shown in Figure 4 as a representative example. In each case, the mutation was found to occur on the normal haplotype.

In this report, we demonstrate that a second focal manifestation of ADPKD is associated with somatic inactivation of the normal *PKD1* allele. We have used novel methods to address several issues raised in response to our initial findings in renal cysts. Our data suggest that with the use of adequately sensitive techniques, it is possible to detect inactivating mutations in a large fraction of cysts. The loss of *PKD1* alone appears to be sufficient for cyst formation since these mutations are intragenic and do not disrupt *TSC2*. Additional support for this model comes from the nonrandom pattern of somatic inactivation that has been observed. In all cysts for which the haplotype could be defined, including those previously described in the literature, it has been the normal allele that was lost or mutated (14/14) (Qian et al., 1996; Brasier and Henske, 1997). Finally, our data are consistent with the results of a recent gene targeting

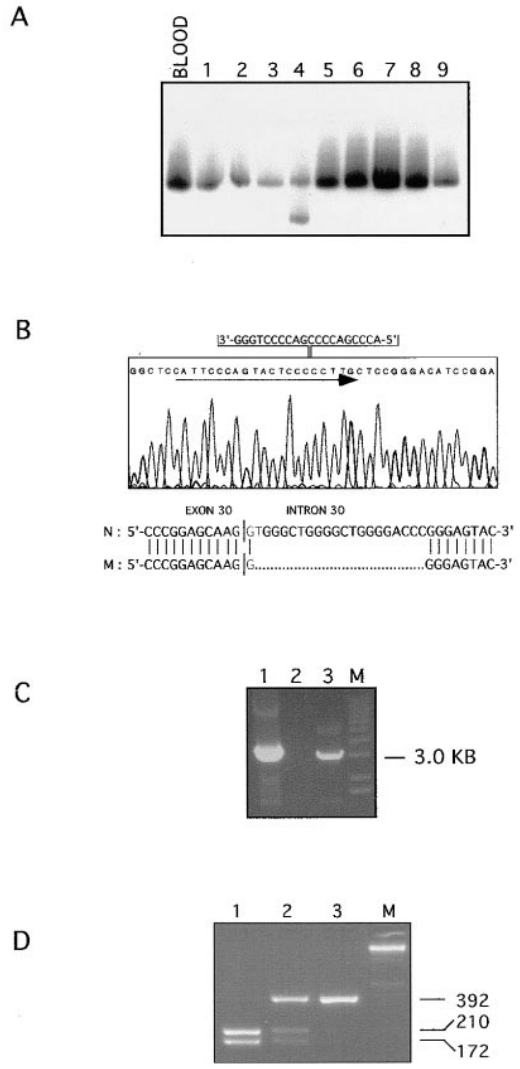

Figure 4. C4 Contains a 20 bp Deletion on the Normal Haplotype that Disrupts a Consensus Splice Site in Intron 30

(A) Intron-based primers were used to amplify exon 30 from the 3′LR of JHU452 and nine individual cysts. The radiolabeled PCR products were subjected to heteroduplex analysis. C4 contains a novel heteroduplex pattern.

(B) A PCR product spanning exons 25–30 was amplified from the 3′LR of C4. This product was cloned and sequenced, and a 20 bp deletion was identified at the exon 30 splice donor site. The sequence of the mutant allele is demonstrated in the reverse orientation, and the deleted base pairs are noted. To clarify the effect of this mutation, the sequences of normal (N) and mutant (M) alleles are noted below in the forward orientation. The vertical bar identifies the position of the exon/intron boundary for the end of exon 30. The dashes represent the deleted base pairs. The arrow shows the sequence of a primer that was designed to amplify only the mutant allele.

(C) The "mutant"-specific primer was used to amplify a PCR product of ~3 kb spanning exons 25–30 directly from cyst DNA (lane 3). This primer would not support amplification from either the blood (lane 2) or the 3′LR (data not shown) of JHU452. A clone with the deletion (lane 1) is included as a positive control. This demonstrates the specificity of the primer and suggests that the deletion was a somatic event not present in the germline of JHU452.

(D) Exon 25 was amplified from the mutant-specific PCR product shown in (C) (lane 3), a clone containing the *PG2* polymorphism (lane 1), and the 3′LR of JHU452 (lane 2). The products were digested with MspI and analyzed on a Nusieve gel. Exon 25 amplified from the mutant-specific product did not cut with MspI, indicating that the PCR product does not contain *PG2*. Since this polymorphism segregates with the disease phenotype in the family of JHU452, the deletion occurred on the normal haplotype. The mutant-specific PCR product was diluted to $1:10^4$ for nested amplification of exon 25 to ensure that there was no contamination of cyst DNA (data not shown).

study of murine *PKD1*. In this model, only homozygous mice developed cysts (Lu et al., 1997).

Collectively, these data support a recessive molecular model for ADPKD, Type I. Most, if not all, cysts are likely to be comprised of a unique combination of germline and somatic mutations. It is reasonable to speculate that all focal manifestations of the disease result from a similar process. The factors governing the rate of second hits have yet to be defined and may involve a combination of genetic and environmental determinants.

Experimental Procedures

Preparation of Cyst DNA

DNA was prepared from the individual liver cysts of two donors (JHU415 and JHU452) using techniques described in detail elsewhere (Qian et al., 1996). Briefly, the contents of each cyst were drained using a needle/syringe, and the needle was left in the cyst for the duration of the procedure. The cavity of the cyst was rinsed a minimum of three times with Ca^{2+}- and Mg^{2+}-free PBS. Then, PBS containing 2 mM EDTA was injected into the lumen of the cyst and incubated for 20 min. The cyst contents were collected and the DNA extracted using the Puregene DNA extraction kit (Gentra).

EJ1 Analysis of JHU415

The polymorphic locus *EJ1* was identified by heteroduplex analysis of a PCR product containing a portion of exons 45 and 46 as well as the intervening intron (Qian et al., 1996). *EJ1* is amplified using the primers FQF28 (5′-CACGCCTTGCGTGGAGAG-3′) and FQR35 (5′-ATGGGCCACGGGAAGATCC-3′). The sequence of the three alleles, A1–A3, that account for the polymorphism has been previously reported along with methods for performing mixing studies with cloned alleles (Qian et al., 1996). The *EJ1* alleles from the blood DNA of JHU415 and C11 were cloned into pCRII (Invitrogen). Two independent clones containing each allele were sequenced using an ABI automated sequencer. To test for the presence of the germline *Mae*I site, a nested PCR product of 329 bp was amplified using primers FQF28 and C12R1 (5′-GAGGTGGAGGGGTGCGAG-3′). The *Bst*UI site in C11 was also assayed using a nested product of 391 bp amplified using primers C12F1 (5′-CTCTGCCCAGGGTGCAGC-3′) and FQR35.

Long-Range PCR

300 ng of genomic DNA (isolated from whole blood using the Puregene kit) or 5 μl of cyst DNA was used as template for amplification of two long-range, gene-specific templates, 3′LR and 5′MR. The PCR conditions and primer sequences used to generate 3′LR (~10 kb) have been published elsewhere (Watnick et al., 1997). 5′MR (~3 kb) was amplified using a *PKD1*-specific primer (FQF26, 5′-AGCGC AACTACTTGGAGGCCC-3′) located in exon 15 and another primer (TWR2, 5′-GCAGGGTGAGCAGGTGGGGCCATCCTA-3′) located in intron 21 prior to the polypyrimidine tract in that intron. The specificity of 5′MR was verified using strategies reported previously for 3′LR (Watnick et al., 1997). The PCR conditions for 5′MR are as follows: 95°C for 3 min, 35 cycles of 95°C for 20 s, and 70°C for 4 min and a final extension of 72°C for 10 min. The total PCR volume was 50 μl using 4 U of r*Tth* DNA polymerase XL (Cetus, Perkin Elmer) and a final Mg^+ concentration of 1.1 mM. The long-range templates were serially diluted to ($1:10^4$ or $1:10^5$) to remove genomic contamination.

Mutation Analysis

2 μl of diluted template (1:10^4–1:10^5) was used for amplification of individual exons 23–34 (3′LR) or exons 16–21 (5′MR). The primer sequences used for amplification of exons 23–34 have been published (Watnick et al., 1997). Intron-based primers were similarly designed for exons 16–21 (our unpublished data). PCR was performed using 2 U of *Taq* DNA polymerase (Boerhringer Mannheim) and 0.2 μl of dCTP in a 30 μl reaction volume. The radiolabeled PCR products were then subjected to heteroduplex analysis using Hydrolink Mutation Detection enhancement gels (MDE, AT Biochem). Exons harboring variants were either cloned and sequenced as above or the PCR products were prepared for direct sequencing (Thermosequenase, Amersham) using microcon columns (Amicon). All sequence variants were confirmed by restriction digest in a second long-range template. In addition, we tested for the presence of each variant in the homologous loci using the cell line, N23HA, and total blood DNA (Germino et al., 1990; The European Polycystic Kidney Disease Consortium, 1994).

Haplotype Analysis for JHU452

The haplotype on which each mutation occurred was determined in one of several ways. For the C8 stop codon in exon 19, cloned fragments linking exon 17 to 19 were analyzed for the presence of *PG1* or the exon 19 stop codon. The remaining cysts were analyzed using primers that could distinguish between mutant and normal alleles as described in the text. Conditions for PCR were optimized using clones that contained mutant or normal sequences, and the blood DNA of JHU452 was always used as a negative control. In the case of C4, the primer (5′-CATTCCCAGTACTCCCCCTTG-3′) was designed to span the deletion breakpoint in exon 30 (Figure 4). Alternatively, for C2 a primer specific for the exon 24 stop codon was designed (5′-AGGATCCGCCCAGAGGG-3′) by placing the C-to-G mismatch at the 3′ end of the primer and introducing another intentional mismatch (T-to-G) at the second 3′ base pair. The intentional mismatch was chosen to destabilize primer binding to the "normal sequence" using established guidelines (Kwok et al., 1990). The presence of a local sequence reduplication around the C9 exon 23 deletion, however, precluded the design of a mutant-specific primer. Instead a primer specific for the normal allele was synthesized (5′-GTCACCCTGGACAGCAGCA-3′) with the presumption that the deletion would have occurred on the opposite background. Since the primer was specific for "normal" sequence, haplotype was determined from the diluted 3′LR to avoid amplification from homologous loci.

Acknowledgments

We are extremely grateful to all family members for their invaluable participation. We thank Ms. Sidney McGaughey and Dr. Klaus Piontek for their assistance in the preparation of the manuscript. This work was supported by grants from the National Institutes of Health (G. G. G., DK48006; V. T., DK44863; K. W. K., DK48532); the JHU Institutional Solo Cup Award (T. W.); the Polycystic Kidney Research Foundation (T. W.); and the McCutcheon Foundation (G. G. G.). G. G. G. is the Irving Blum Scholar of The Johns Hopkins University School of Medicine.

Received April 20, 1998; revised June 14, 1998.

References

The American PKD1 Consortium (1995). Analysis of the genomic sequence for the autosomal dominant polycystic kidney disease (PKD1) gene predicts the presence of a leucine-rich repeat. Hum. Mol. Gen. *4*, 575–582.

Brasier, J.L., and Henske, E.P. (1997). Loss of the polycystic kidney disease (*PKD1*) region of chromosome 16p13 in renal cyst cells supports a loss-of-function model for cyst pathogenesis. J. Clin. Invest. *99*, 194–199.

Brook-Carter, P.T., Peral, B., Ward, C.J., Thompson, P., Hughes, J., Maheshwar, M.M., Nellist, M., Gamble, V., Harris, P.C., and Sampson, J.R. (1994). Deletion of the TSC2 and PKD1 genes associated with severe infantile polycystic kidney disease—a contiguous gene syndrome. Nat. Genet. *8*, 328–332.

The European Polycystic Kidney Disease Consortium (1994). The polycystic kidney disease gene encodes a 14 kb transcript and lies within a duplicated region on chromosome 16. Cell *77*, 881–894.

Everson, G.T. (1993). Hepatic cysts in autosomal dominant polycystic kidney disease. Am. J. Kid. Dis. *22*, 520–525.

Gabow, P.A. (1993). Autosomal dominant polycystic kidney disease. N. Engl. J. Med. *329*, 332–342.

Germino, G.G., Barton, N.J., Lamb, J., Higgs, D.R., Harris, P., Scherer, G., Nakamura, Y., and Reeders, S.T. (1990). Identification of a locus which shows no genetic recombination with the autosomal dominant polycystic disease gene on chromosome 16. Am. J. Hum. Genet. *46*, 925–933.

Germino, G.G., Weinstat-Saslow, D., Himmelbauer, H., Gillespie, G.A.J., Somlo, S., Wirth, B., Barton, N., Harris, K.L., Frischauf, A.-M., and Reeders, S.T. (1992). The gene for autosomal dominant polycystic kidney disease lies in a 750 kb CpG-rich region. Genomics *13*, 144–151.

Iglesias, C.G., Torres, V.E., Offord, K.P., Holley, K.E., Beard, C.M., and Kurland, L.T. (1983). Epidemiology of adult polycystic kidney disease, Olmstead County, Minnesota: 1935–1980. Am. J. Kidney. Dis. *2*, 630–639.

Kaehny, W.D., and Everson, G.T. (1991). Extrarenal manifestations of autosomal dominant polycystic kidney disease. Semin. Nephrol. *11*, 661–670.

Kwok, S., Kellogg, D.E., McKinney, N., Spasic, D., Goda, L., Levenson, C., and Sninsky, J.J. (1990). Effects of primer-template mismatches on the polymerase chain reaction: human immunodeficiency virus type 1 model studies. Nucleic Acids Res. *18*, 999–1005.

Lu, W., Peissel, B., Babakhanlou, H., Pavlova, A., Geng, L., Fan, X., Larson, C., Brent, G., and Zhou, J. (1997). Perinatal lethality with kidney and pancreas defects in mice with targeted PKD1 mutation. Nat. Genet. *17*, 179–181.

Mochizuki, T., Wu, G., Hayashi, T., Xenophontos, S.L., Veldhuisen, B., Saris, J.J., Reynolds, D.M., Cai, Y., Gabow, P.A., Pierides, A., et al. (1996). PKD2, a gene for polycystic kidney disease that encodes an integral membrane protein. Science *272*, 1339–1342.

Ong, A.C., and Harris, P.C. (1997). Molecular basis of renal cyst formation—one hit or two? Lancet *349*, 1039–1040.

Peral, B., Sanmillan, J.L., Ong, A.C.M., Gamble, V., Ward, C.J., Strong, C., and Harris, P.C. (1996). Screening the 3′ region of the polycystic kidney disease 1 (PKD1) gene reveals six novel mutations. Am. J. Hum. Genet. *58*, 86–96.

Peters, D.J.M., and Sandkuijl, L.A. (1992). Genetic heterogeneity of polycystic kidney in Europe. Contrib. Nephrol. *97*, 128–139.

Qian, F., Watnick, T.J., Onuchic, L.F., and Germino, G.G. (1996). The molecular basis of focal cyst formation in human autosomal dominant polycystic kidney disease type 1. Cell *87*, 979–987.

Qian, F., Germino, F.J., Cai, Y., Zhang, X., Somlo, S., and Germino, G.G. (1997). PKD1 interacts with PKD2 through a probable coiled-coil domain. Nat. Genet. *16*, 179–183.

Snarey, A., Thomas, S., Schneider, M.C., Pound, S.E., Barton, N., Wright, A.F., Germino, G.G., Somlo, S., Harris, P.C., Reeders, S.T., and Frischauf, A.-M. (1994). Linkage disequilibrium in the region of the autosomal dominant polycystic kidney disease gene (PKD1). Am. J. Hum. Genet. *55*, 365–371.

Tsiokas, L., Kim, E., Arnould, T., Sukhatme, V.T., and Walz, G. (1997). Homo- and heterodimeric interactions between the gene products of PKD1 and PKD2. Proc. Natl. Acad. Sci. USA *94*, 6965–6970.

Watnick, T.J., Piontek, K.B., Cordal, T.M., Weber, H., Gandolph, M.A., Qian, F., Lens, X.M., Neumann, H.P.H., and Germino, G.G. (1997). An unusual pattern of mutation in the duplicated portion of *PKD1* is revealed by use of a novel strategy for mutation detection. Hum. Mol. Genet. *6*, 1473–1481.